*Int. J. Electrochem. Sci.*, 4 **(2009)** 1628 - 1637

**International Journal of ELECTROCHEMICAL SCIENCE**
www.electrochemsci.org

# Vertically Aligned CdSe and Zn-doped CdSe Nanorod Arrays Grown Directly on FTO Coated Glass: Synthesis and Characterization

*D. Soundararajan, J.K. Yoon, Y.I. Kim, J.S. Kwon, C.W. Park, S.H. Kim, J.M. Ko**

Division of Applied Chemistry & Biotechnology, Hanbat National University, San 16-1, Dukmyung-Dong, Yusung-Gu, Daejeon 305-719, South Korea
*E-mail: jmko@hanbat.ac.kr

*Received:* 19 September 2009 / *Accepted:* 1 December 2009 / *Published:* 31 December 2009

Vertically aligned nanorod arrays of CdSe and Zn doped CdSe films were grown on FTO coated glass substrate by using cathodic electro deposition method. The composition, crystal structure, surface morphology and optical properties of the as-grown pure CdSe and Zn doped CdSe nanotubular films were examined by using energy dispersive spectroscopy, x-ray diffractometer, field emission scanning electron microscope, UV-Vis-IR spectrophotometer and photoluminescence techniques, respectively. XRD study showed the hexagonal crystal structure without any precipitates related to Zn. SEM images clearly showed end capped vertically aligned nanorods arranged closely. The optical transmittance spectra were recorded within the range of 300-1000 nm. The band gap energy was found to vary between 1.94 and 1.98 eV due to the incorporation of Zn. PL spectra showed a narrow near band gap emission at 1.81 and 1.94 eV for CdSe and Zn doped CdSe nanorod arrays.

**Keywords:** CdSe and CdSe:Zn Nanorod arrays; Optical properties; Cathodic Electrodeposition

## 1. INTRODUCTION

Controlled synthesis of nanostructured materials with desired shape and size is technologically important [1, 2]. One dimentional nanostructures of semiconductors have attracted widespread attention because of their special structure, optical, and electronic transport properties arising from the quantum confinement of electrons and high surface to volume ratio [3, 4]. Such 1D semiconductor nanostructues show size dependent structural, morphological, optical and electrical properties, which make them potential candidates for different applications such as solar cells, light emitting diodes and field emitters [5-7]. Development of such materials, whose structural, morphological and optoelectronic properties can be tuned, are useful in many applications. For example, optoelectronic

devices particularly, solar cell devices can be modified accordingly. Nanorods of II-VI compound semiconductors and their metal chalcogenides are getting special attention due to the tunable bandgap by doping and morphology control [8]. The research on CdSe and Zn doped CdSe nanostructures is getting attention due to its potential use as inorganic sensitized metal oxide solar cells [9-11]. The size effect and doping by Zn can tune band gap of CdSe nanostructures and which can vary its optical response from the infrared region to the ultraviolet region and it favor the photocurrent conversion efficiency when used as inorganic sensitizer [12]. Among various nanostructures, the growth of vertically aligned one diementional nanorods/nanowires is one of the major challenges. Sofar, several kinds of techniques have been utilized to fabricate nanoscale materials, such as molecular beam epitaxy [13], sputtering [14], chemical vapor deposition [15], spray pyrolysis [16], pulsed laser deposition [17], anodic alumina oxide (AAO) template [18], cathodic electrodeposition [19] and aqueous solution deposition methods [20]. Among various methods, cathodic electrodeposition technique is emerged as a competitive technique for the fabrication of nanostructured semiconducting films. Significant advantages of this method are controllable size, morphology, composition, low temperature growth, cost-effectiveness, and less complicated. In the present work, we report the growth of vertically aligned arrays of CdSe and Zn doped CdSe nanorods directly on FTO coated glass substrate and discuss its structure, composition, morphology and optical properties.

## 2. EXPERIMENTAL PART

### *2.1. Preparation of CdSe and Zn doped CdSe nanorod arrays*

$Cd_{1-x}Zn_xSe$ (x = 0.0, 0.3) films were electrodeposited onto fluorine doped tin oxide (FTO) film coated glass substrate at 26°*C* by using an aqueous bath. Cadmium acetate [$Cd(CH_3COO)_2$], zinc acetate [$Zn(CH_3COO)_2$] and selenium dioxide ($SeO_2$) were used as source of Cd, Zn and Se, respectively. The solutions of cadmium acetate, zinc acetate, selenium dioxide were mixed in proper proportion according to the composition. Chronopotentiometric technique with constant current density having three-electrode system viz. working, counter, and reference was used with computer based Potentiostat. Well cleaned working FTO coated glass, Pt counter and Ag/AgCl reference electrodes were used. A constant current density of –2 mA/cm$^2$ was applied for 20 minutes between working FTO and Pt counter electrodes in the presence of Ag/AgCl reference electrode.

### *2.2. Characterization*

After deposition, the film coated substrates were taken out of the bath, rinsed with deionized water, dried in air and kept in an airtight plastic container. The elemental composition was determined using an Energy dispersive x-ray analysis (EDS) attached to the Field emission scanning electron microscope (JEOL, JSM-6300). The film thickness and morphological analysis was performed by using FE-SEM. Structure of the grown films was done by using powdered X-ray diffraction technique (XRD - Rigaku, D/MAX 2500H) using a Cu$K\alpha$ source radiation. The diffractometer was operated in

the step scan mode with a step of 0.02 and in the 2Θ range of 20°–70°. The optical transmittance spectra were obtained within the spectral range 300-1000 nm using a UV-vis-spectrophotometer (HP-8453). The luminescence spectra were recorded by using a photoluminescence spectrometer (LS-50 B) with Xenon flash lamp as light source.

## 3. RESULTS AND DISCUSSION

### *3.1. Chronopotentiometry*

Chronopotentiometry is an electrochemical technique in which a dilute unstirred solution of an electroactive species, in the presence of an excess of a supporting electrolyte, is subjected to a constant current electrolysis and the variations of the working electrode potential, against a suitable non-polarizable reference, are recorded as a function of time. The reduction of $Cd^{2+}$, $Zn^{2+}$ and $Se^{2-}$ on a FTO working electrode from its solutions was investigated by recording chronopotentiograms. Typical chronopotentiograms for the electrodeposition of CdSe and Zn doped CdSe nanorod array films under a constant current density of -2 mA/cm$^2$ at a temperature of 26°C are shown in Fig. 1(a-b). It is seen from Fig 1a that the chronopoteniometric transient of CdSe shows a small swallow in the beginning, indicating the reduction of Cd and Se ions. In the case of Zn doped CdSe, a large swallow in the beginning of transient indicates the reduction of Cd, Zn and Se ions as shown in Fig 1b. In addition, smaller swallows at more cathodic potentials are also noticed for short time elapse during the deposition of zinc from the solution. This implies the incorporation of Zn into CdSe lattice.

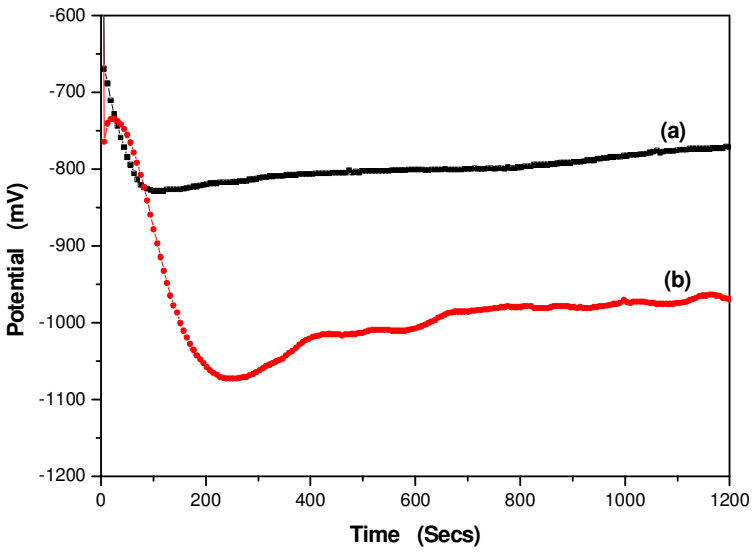


**Figure 1.** Chronopotentiograms of electrodeposition of (a) CdSe and (b) Zn doped CdSe films.

*3.2. EDS spectra*

Figs.2(a,b) shows the EDS spectra of CdSe and Zn doped CdSe films. Strong peaks for Cd and Se were found in the spectrum as the concentrations of these elements were high compared to that of Zn. Inset shows the relative atomic percentage of Cd, Se and Zn. The elemental composition of the films and the initial values in the reaction bath were similar, within an error limit of ±1%.

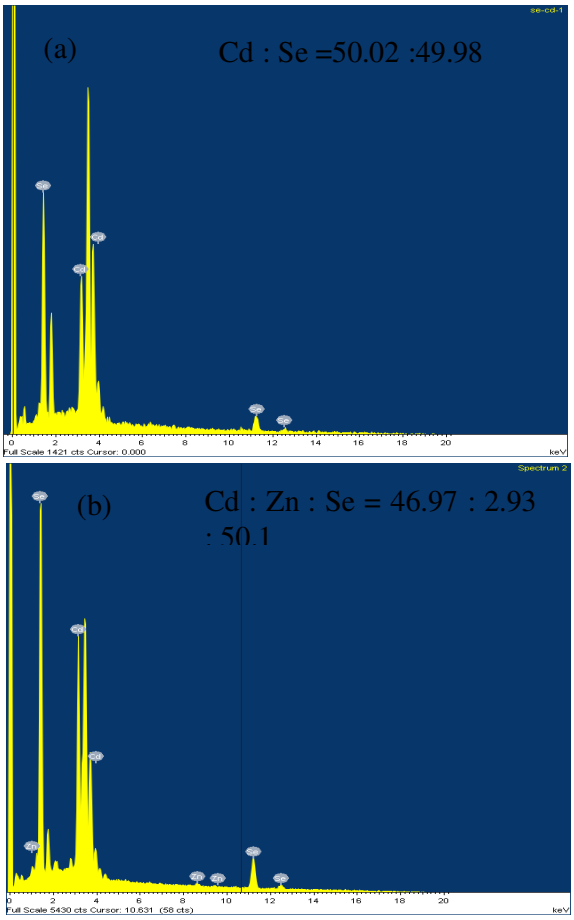


**Figure 2.** EDS spectrum of (a) CdSe and (b) Zn doped CdSe films.

*3.3. XRD analysis*

X-ray diffraction patterns of CdSe and Zn doped CdSe films grown on FTO coated glass substrate in the 2$\theta$ scan range of 20° to 70° are shown in Fig.3(a-b). Diffraction pattern of CdSe shows peaks at 2$\theta$ angles of 25.54°, 26.35°, 38.28° and 51.38° along (100), (002), (100), (102) and (004) crystallographic directions indicate the hexagonal crystal structure [21, 22]. Further, similar reflections such as (002), (100), (102) and (004) that characterize hexagonal structure were noticed for Zn doped CdSe. The diffraction peaks are not shifted in the Zn doped CdSe (relative to the undoped CdSe)

presumably because of the rather low doping levels. Interestingly, the as-obtained vertically aligned CdSe and Zn doped CdSe nanorod array films showed good crystallinity without any Zn related secondary phases. However, a minute amorphous phase of CdSe and selenium precipitate were noticed at 42.23° and 47.9°, respectively.

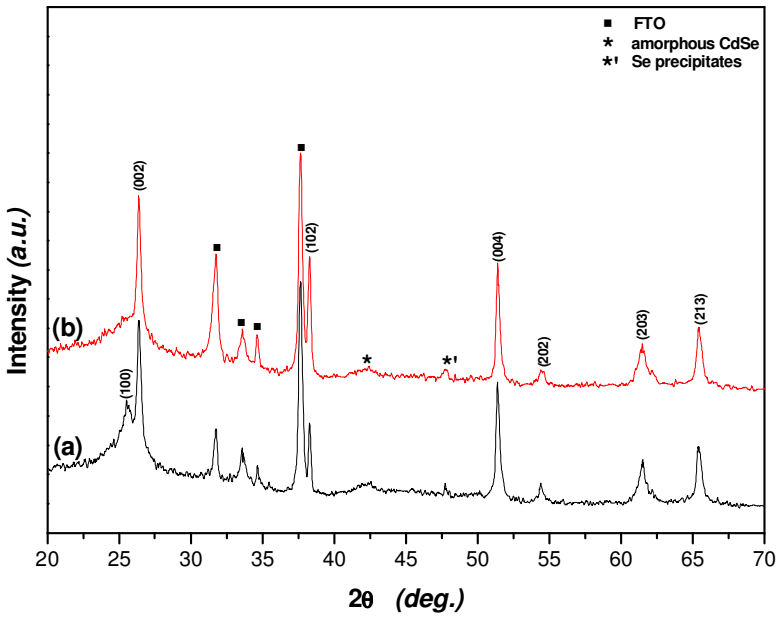


**Figure 3.** X-ray diffraction patterns of (a) CdSe and (b) Zn doped CdSe films grown on FTO coated glass substrate.

Microstructural parameters such as particle size, lattice constant, strain and dislocation density of CdSe and Zn doped CdSe films were evaluated from the diffraction patterns.

The crystalline size ($D$) is calculated using the Scherrer formula from the full-width at half maximum (FWHM) $\beta$ [23]:

$$D = (0.94 \times \lambda)/(\beta \times \cos\theta) \quad (1)$$

Where '$\lambda$' is the wavelength of the X-ray used, '$\beta$' is the FWHM in radians, '$D$' is the particle size and $\theta$ is the angle between the incident and the scattered X-ray.

The strain ($\varepsilon$) values can be evaluated by using the following relation [23]:

$$\varepsilon = \beta \cos\theta / 4 \quad (2)$$

The lattice spacing ($d$) is calculated from the Bragg's formula, $d = \lambda/(2\sin\theta)$. The lattice parameters '$a$' and '$c$' are determined for hexagonal structure by the following expression [24]:

$$1/d^2 = 4/3a^2(h^2 + hk + k^2) + (l^2/c^2) \quad (3)$$

Where h, k and l represent the lattice planes. The dislocation density ($\delta$) has been calculated by using the following relation [24]:

$$D = 15\beta\cos\theta / 4aD \quad (4)$$

The structural parameters for CdSe and Zn doped CdSe films are given in Table 1. The calculated values of lattice spacing and lattice parameter show good agreement with the standard card (JCPDS Card File No: 77-2307). Scherrer analyses of these XRD data shows a decrease in grain size from 39.56 to 32.94 nm with Zn doping. Also the evaluated values of strain and dislocation density are tends to decrease from $120.6\times10^{-3}$ to $111.06\times10^{-3}$ $lin^{-2}$ $m^{-4}$ and from 26.2 to $12.73\times10^{15}$ lin $m^{-2}$ with Zn doping. This may be due to the improvement in the crystallinity of the film with Zn doping.

**Table 1.** Microstructural and optical properties of CdSe and Zn doped CdSe nanotubular films

| Samples | 2θ (*deg.*) | *h k l* | *Crystal* structure | Lattice spacing d (*Å*) | Lattice parameter *a* (*Å*) | Particle size D (*nm*) | *Strain*×$10^{-3}$ ε ($lin^{-2}$ $m^{-4}$) | *Dislocation* density×$10^{15}$ lin $m^{-2}$ | *Band gap* (*eV*) |
|---|---|---|---|---|---|---|---|---|---|
| CdSe | 25.54 | 100 | HP | 0.348 | a = 0.402 | 39.56 | 120.6 | 26.2 | 1.94 |
| | 26.35 | 002 | | 0.338 | c = 0.676 | | | | |
| | 38.28 | 102 | | 0.235 | | | | | |
| | 51.38 | 004 | | 0.177 | | | | | |
| CdSe:Zn | - | - | HP | - | | 32.94 | 111.06 | 12.73 | 1.98 |
| | 26.35 | 002 | | 0.338 | | | | | |
| | 38.28 | 102 | | 0.235 | | | | | |
| | 51.38 | 004 | | 0.177 | | | | | |

*HP – Hexagonal phase

### *3.3. SEM micrographs*

The plane and cross sectional views of SEM images of CdSe and Zn doped CdSe films are shown in Fig 4(a-d). The plane view shows capped granular like morphology which is nothing but the top outlook of the nanorod arrays. The cross sectional images showed closed arranged vertically aligned nanorod arrays. In case of CdSe, the nanorod arrays look grainy and the rods are not smooth. On the other hand, in the case of Zn doped CdSe, the nanorod arrays are smooth. In both cases, the average length of the nanorod is around 500 nm and is not changed with the doping of Zn. However, the average value of nanorod diameter has been noticed to decrease from 200 to 160 nm with Zn doping. Upon comparing the cross sectional views of CdSe and Zn doped CdSe nanorod array films, it is also clear that the CdSe is relatively rich in voids, cracks and any other serious defects than the Zn doped CdSe.

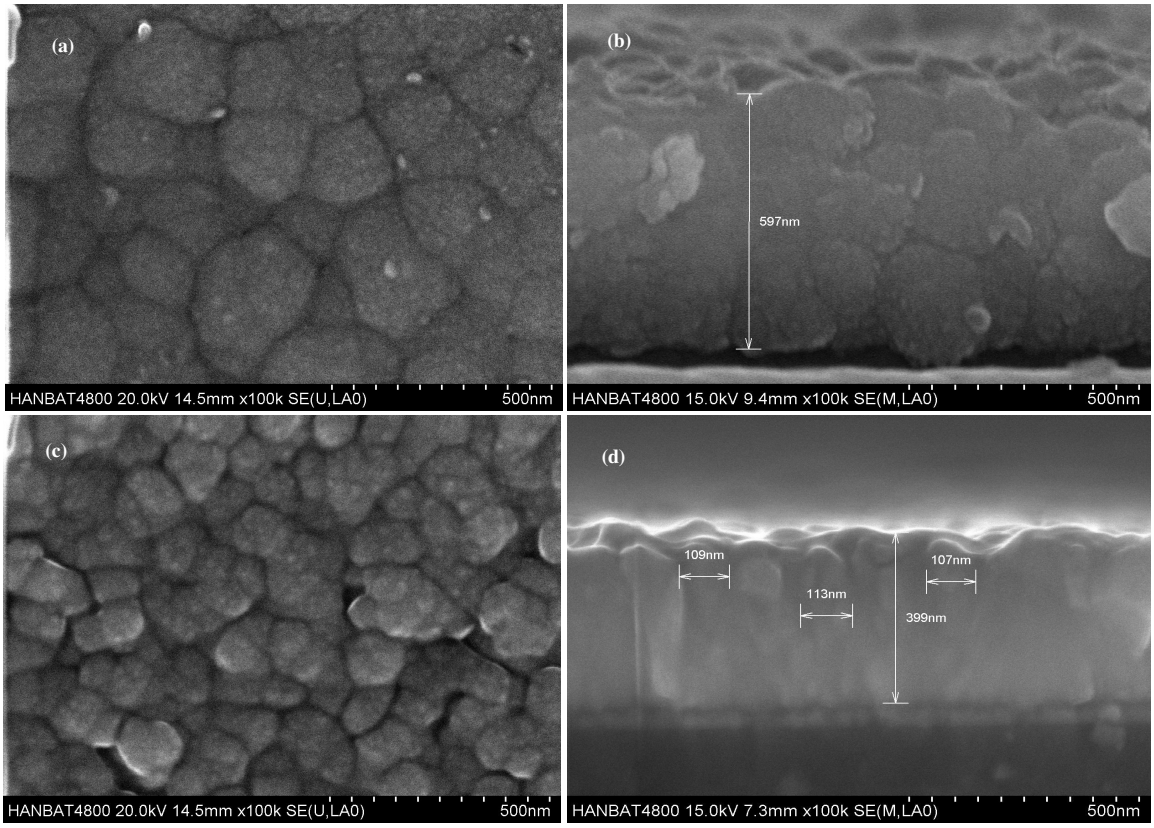


**Figure 4.** FE-SEM images of CdSe film in (a) plane and (b) cross sectional view and Zn doped CdSe film in (c) plane and (d) cross sectional view.

### *3.4. Optical studies*

#### *3.4.1. Transmittance spectra*

After discussing the structure and morphological studies, we analyze optical properties that are fundamental for the performance of nanostructured solar cells. Transmittance studies were carried out in the wavelength range of 300–1000 nm to investigate the optical absorption properties of the CdSe and Zn doped CdSe nanorod array films. The obtained results are plotted in Fig. 5(a-b). CdSe and CdSe:Zn nanorod arrays show a change in optical transmittance. These changes are attributed to structural, compositional, crystallinity and morphological changes taking place when Zn is incorporated into CdSe lattice. Fundamental absorption edge is found to shift towards lower wavelength region (from 736 to 675 nm) when Zn has been introduced into CdSe host lattice. The cause of observed blue shift shall be due to the decrease of Cd concentration and increase of Zn concentration in the films. This is because the bandgap of ZnSe is greater than that of CdSe. The absorption coefficients are calculated using the relation, $\alpha = \frac{2.303\log(1/T)}{d}$, where d is film thickness and T is transmittance. The band gap value has been obtained by the plot between $(\alpha h\nu)^2$ and photon energy ($h\nu$) as shown in the inset of Fig. 5. The plot between $(\alpha h\nu)^2$ and $h\nu$ is found to have straight

line over any part of the optical absorption spectrum, thus supporting the interpretation of direct allowed transition [25]. Extrapolation of the linear portion of the curve to $(\alpha h\nu)^2 = 0$ gives the optical band gap value for the films. It is observed that the direct band gap energy for undoped CdSe film is 1.94 and it increases to 1.98 eV for Zn doped CdSe film.

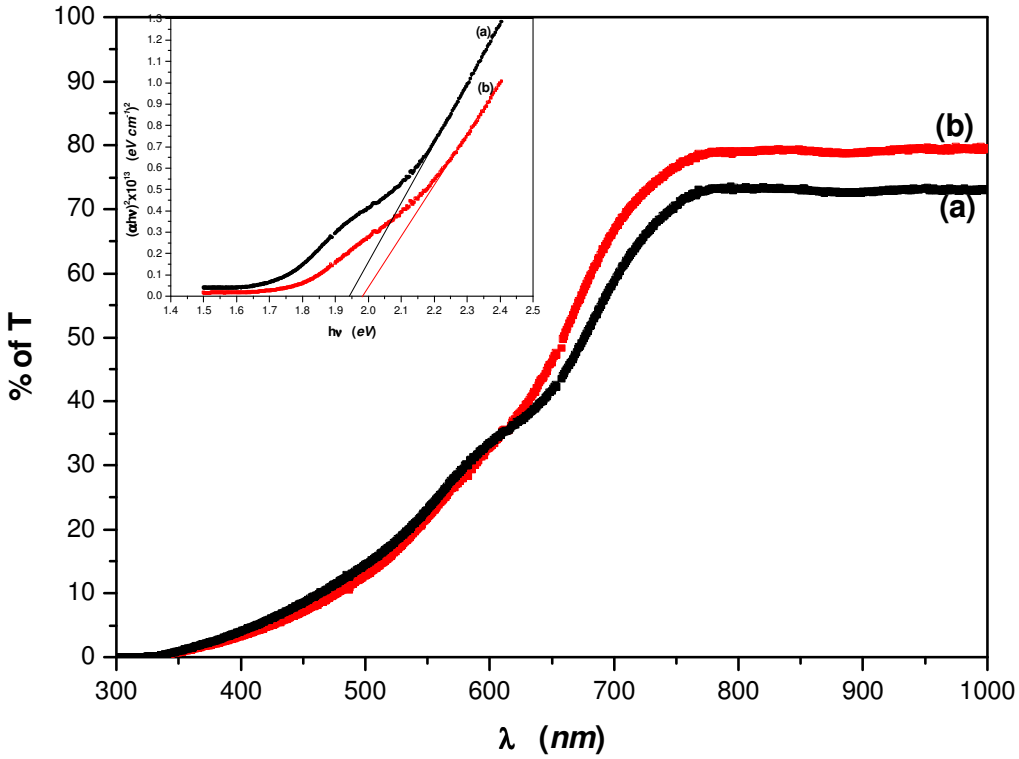


**Figure 5.** Transmittance spectra of (a) CdSe and (b) Zn doped CdSe films. Inset shows the plot between $(\alpha h\nu)^2$ and hν. The obtained value of band gap of CdSe and CdSe:Zn are 1.94 and 1.98 eV, respectively. .

### *3.4.2. Photoluminescence spectra*

The photoluminescence (PL) experiment was employed to study the optical response of CdSe and Zn doped CdSe films, and the spectrum taken at room temperature is shown in Fig. 6(a-b). The CdSe and Zn doped CdSe films were excited at 340 and 320 nm of Xe flash lamp and recorded in the wavelength range from 500 to 800 nm. The PL spectra of CdSe and Zn doped CdSe exhibit a narrow peak at around 681.68 and 638.57 nm, respectively. The narrow peaks result from free exciton emission and are close to the absorption edge of the obtained CdSe and Zn doped CdSe nanorod array films. This type of emission is often called as near-band-edge (NBE) emission. It is noticed that the intensity of PL peak is found to decrease and also line width is found to increase from 49 to 58 *meV* with Zn doping. The shift in the emission line implies increase in band gap with Zn doping. No photoluminescence activity at all measured wavelength region except a narrow NBE shall be due to the

presence of defect-related levels that favor the non-radiative recombination mechanisms instead of the radiative ones at room temperature [26, 27].

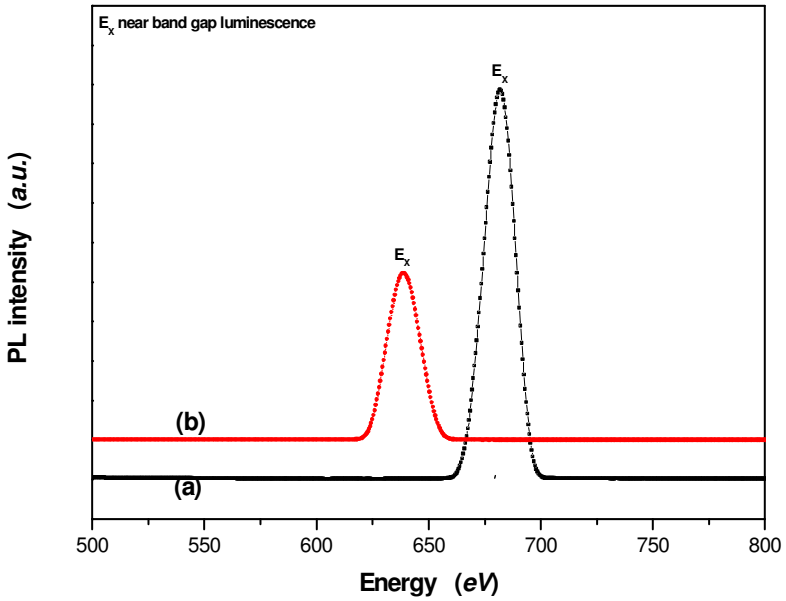


**Figure 6.** Room temperature photoluminescence emission spectra of (a) CdSe and (b) CdSe:Zn films.

## 4. CONCLUSIONS

We have successfully prepared vertically aligned CdSe and Zn doped CdSe nanorod array films directly on FTO coated glass substrate by using a simple cathodic electrodeposition method in chronopotentiometric mode (-2 mA/cm$^2$, 20 min) at a low temperature of 26 $^{\circ}C$. Structural investigation by XRD has shown that the as-deposited films are hexagonal nature. Crystalline quality is found to increase with Zn doping and no detectable secondary phase corresponding to Zn related precipitates is observed. FE-SEM images clearly showed closely arranged vertically aligned nanorod arrays and it also indicated the Zn addition has improved the alignment of nanorods. The band gap values have shown to increase from 1.94 to 1.98 eV with Zn doping. Room temperature PL spectra with a narrow near band edge emission peak have confirmed the fine crystalinity of the as-obtained vertical nanorod arrays with non radiative recombination mechanism of defect related levels. Further investigations are under research, which aims to improve well aligned vertical nanorods by means of using a thin nano CdSe as buffer layer.

ACKNOWLEDGMENTS
This work was supported by the World Class University Program (R33-2008-000-10147-0) from Ministry of Education, Science and Technology, Korea.

**References**


1. J.P. Kar, M. Kumar, J.H. Choi, S.N. Das, S.Y. Choi, J.M. Myoung, *Solid State Communications. 149 (2009) 1337-1341*
2. Z.H. Zhang, X.Y. Qi, J.K. Jian, X.F. Duan, *Micron. 37 (2006) 229-233*
3. D.L. Klein, R. Roth, A.K.L. Lim, A.P. Alivisatos, P.L. McEuen, *Nature.* 389 (1997) 699.
4. A. Henglein, *Chem. Rev.* 89 (1989) 1861.
5. Minsung Jeon, Koichi Kamisako, *Materials Letters.* 63 (2009) 777-779
6. [6] Lei Luo, Yanfeng Zhang, Samuel S. Mao, Liwei Lin, Sensors and Actuators A: Physical. 127 (2006) 201-206
7. Farid Jamali Sheini, Dilip S. Joag, Mahendra A. More, *Ultramicroscopy.* 109 (2009) 418-422
8. Sun-Ki Min, Oh-Sim Joo, Kwang-Deog Jung, Rajaram S. Mane, Sung-Hwan Han, *Electrochemistry Communications. 8 (2006) 223-226*
9. Ramon Tena-Zaera, Margaret A. Ryan, Abou Katty, Gary Hodes, Stéphane Bastide, Claude Lévy-Clément, *Comptes Rendus Chimie. 9 (2006) 717-729*
10. S.D. Chavhan, R.S. Mane, Wonjoo Lee, S. Senthilarasu, Sung-Hwan Han, J. Lee, Soo-Hyoung Lee, *Electrochimica Acta. 54 (2009) 3169-3175*
11. Ju-Hyun Ahn, R.S. Mane, V. V. Todkar and Sung-Hwan Han, *Int. J. Electrochem. Sci.,* 2 (2007) 517 – 522
12. Qing Shen, Tadakazu Sato, Mituru Hashimoto, Changchuan Chen, Taro Toyoda, *Thin Solid Films. 499 (2006) 299-305*
13. Y.M. Park, R. Andre, J. Kasprzak, Le Si Dang, E. Bellet-Amalric, *Applied Surface Science. 253 (2007) 6946-6950*
14. Levichev, A. Chahboun, P. Basa, A.G. Rolo, N.P. Barradas, E. Alves, Zs.J. Horvath, O. Conde, M.J.M. Gomes, *Microelectronic Engineering*, *85 (2008) 2374-2377*
15. H. Chenga, H.Y. Chaoa, Y.H. Changa, C.H. Hsua, C.L. Chenga, T.T. Chena, Y.F. Chena, M.W. Chub, *Physica E.* 40 (2008) 2000–2003
16. T. Elango, V. Subramanian, K. R. Murali, *Surface and Coatings Technology*. 123 (2000) 8-11
17. M.A. Hernandez-Perez, J. Aguilar-Hernandez, G. Contreras-Puente, J.R. Vargas-García, E. Rangel-Salinas, Physica E: Low-dimensional Systems and Nanostructures. 40 (2008) 2535-2539
18. Xin Wang, Gao-Rong Han, *Microelectronic Engineering*, 66, (2003) 166-170
19. Mohamed S. El-Deab, *Int. J. Electrochem. Sci.*, 4 (2009) 1329 - 1338
20. Mao-Quan Chu, Ye Sun, Xiao-Yan Shen, Guo-Jie Liu, Physica E: Low-dimensional Systems and Nanostructures. 35 (2006) 75-80
21. Sun-Ki Min, Oh-Sim Joo, Kwang-Deog Jung, Rajaram S. Mane, Sung-Hwan Han, *Electrochemistry Communications. 8 (2006) 223-226.*
22. JCPDS, X-ray powder diffraction file, Joint Committee for Powder Diffraction Standards.
23. S. Venkatachalam, D. Mangalaraj, Sa. K. Narayandass, K. Kim, J. Yi, *Physica B.* 358 (2005) 27–35.
24. R. Murali, B. Jayasuthaa, Solar Energy. 83 (2009) 891-895
25. D. Soundararajan, D. Mangalaraj, D. Nataraj, L. Dorosinskii, J. Santoyo-Salazar, H.C. Jeon, T.W. Kang, *Applied Surface Science. 255 (2009) 7517-7523*
26. N. Chestnoy, T.D. Harris, R. Hull, L.E. Brus, *J. Phys. Chem.* 90 (1986) 3393.
27. Ling Xu, Kunji Chen, Hatim Mohamed El-Khair, Minghai Li, Xinfan Huang, *Applied Surface Science.* 172 (2001) 84-88


© 2009 by ESG (www.electrochemsci.org)